Fast Voltage-Mode Full-Wave Rectifier Using CCII and DXCCII

Jaroslav Koton, Kamil Vrba, and Norbert Herencsar

Brno University of Technology
Dept. of Telecommunications
Technicka 12, 616 00 Brno, Czech Republic
Email: koton@feec.vutbr.cz, vrbak@feec.vutbr.cz, herencsn@feec.vutbr.cz

Abstract

The paper deals with the design and performance analyses of a fast voltage-mode full-wave rectifier. In the structure the second-generation current conveyor and dual-X current conveyor have been used as active elements. The circuit features with maximal simplicity as only two diodes and two resistors are necessary. To enable high-frequency signal processing, current sourcing of the diodes is used with advantage. Using the CMOS implementation of the active elements, the performance of the rectifier was analyzed by evaluating the frequency dependent RMS error and DC transient value for different values of input voltage amplitudes.

1. Introduction

In the area of instrumentation and measurement, the rectifiers serve as very important blocks. They are used in applications such as ac voltmeters and ammeters, signal-polarity detectors, averaging circuits, peak-value detector rectification function is of great importance [1]. The threshold voltage of the diodes does not enable to use simple rectifiers if low-voltage signals are to be analyzed. Therefore, precision rectifiers employing active elements have to be used.

In the circuit theory, the most known solutions of half- or full-wave rectifiers are based on the use of operational amplifiers [1]. As in these circuit solutions the diodes are directly connected to the output of the active element, the finite slew-rate and effects caused by diode commutation from conductive to non-conductive and vice versa state, operate well only at low frequencies, much below the transient frequency of the active element used [2], [3]. An improvement in rectification of high-frequency signal has been achieved by using the supply-current sensing technique, e.g. [4]. As another suitable solution, the current conveyors (CCs) have shown advantageous behavior, where the current sourcing is used, that means the diodes are directly connected to the high-impedance current outputs of the active elements. In [5] the fast full-wave rectifier using two simple second-generation CCs and four diodes is presented.

The behavior of this circuit solution is analyzed in [6]–[8]. To further extend the frequency range the voltage [5], [8] or current [7], [8] biasing scheme can be used. Another precision full-wave rectifier is presented in [9], where the operational amplifiers were replaced by the operational conveyor and by second-generation CC [3]. A full-wave rectifiers using two second-generation or dual-X current conveyors are presented in [10] and [11], respectively, where the required diodes are suitably replaced by NMOS transistors. The main disadvantage of these solution is low accuracy in zero-crossing area (see Fig. 5 in [10], and Fig. 6 in [11]) and in case of [10] the necessity of using two bias voltage sources which have to be equal to the threshold voltage of the NMOS transistors used. The use of fully differential operational transconductance amplifiers (BOTA) operating in weak inversion region for the design of precision full-wave rectifiers is presented in [12]. The solution in [12] is based on the idea discussed in [13], where simple transconductance amplifiers (OTA) are controlled by the current derived from the input signal to be rectified. In another group of precision rectifiers, a transistor connected to the current output of an active element operates as a switch. For this purpose, the current conveyor [14] or transconductance amplifiers [15]–[17] are used.

In this paper, the dual-X current conveyor DXCCII [18] together with simple second-generation current conveyor CCII [19] are with advantage used for the design of minimal configuration fast voltage-mode full-wave rectifier. As passive elements only two didoes and two grounded resistors are required. Using the CMOS implementation of the DXCCII and CCII, the performance of the rectifier is analyzed by evaluating the frequency dependent RMS error and DC transient value for different values of input current amplitudes. Furthermore, SPICE simulations are included showing the feasibilities of the proposed rectifier.

2. CCII and DXCCII Description

Basically, three generations of current conveyors have been described, namely first- (CCI) [20], second- (CCII) [19], and third-generation current conveyor (CCIII) [21]. These active elements are nowadays with advantage used in applications, where wide bandwidth or current output response are necessary. There are different types of CCs that are mostly based on the CCII, e.g. current controlled CC (CCCII) [22], differential voltage CC (DVCC) [23], or electronically tunable CC (ECCII) [24].

The behavior of CCII, which schematic symbol is shown in Fig. 1(a), can be described by the following hybrid matrix:

$$\begin{bmatrix} i_{\mathrm{Y}} \\ v_{\mathrm{X}} \\ i_{\mathrm{Z}} \end{bmatrix} = \begin{bmatrix} 0 & 0 & 0 \\ \alpha_C & 0 & 0 \\ 0 & \beta_C & 0 \end{bmatrix} \begin{bmatrix} v_{\mathrm{Y}} \\ i_{\mathrm{X}} \\ v_{\mathrm{Z}} \end{bmatrix}, \quad (1)$$

where $\alpha_C = 1-\varepsilon_V$ and $\beta_C = 1-\varepsilon_I$ are the voltage and current

---

This research work is funded by projects SIX CZ.1.05/2.1.00/03.0072, GACR P102/09/1681, MSM0021630513, and FEKT-S-11-15.

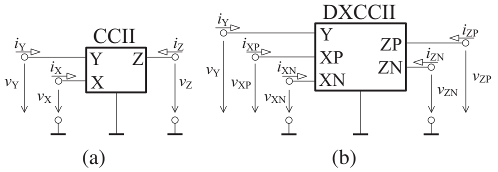

Figure 1. Electrical symbol of the (a) CCII, (b) DXCCII

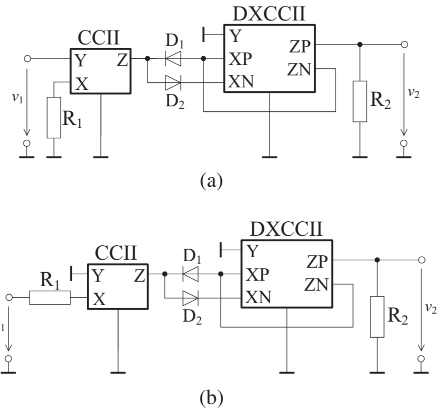

Figure 2. Proposed full-wave rectifiers using DXCCII and CCII featuring with (a) high, (b) low input impedance

transfer ratios of the CCII, whereas $\varepsilon_V \ll 1$ and $\varepsilon_I \ll 1$ are the voltage and current tracking errors, respectively.

In [18] the dual-X second generation CC has been described that conceptually represents a combination of the regular CCII [19] and the inverting second generation current conveyor (ICCII) [25]. The DXCCII (Fig. 1(b)) has two low-impedance current inputs XP and XN. The currents of these terminals are reflected to the high-impedance current outputs ZP and ZN. The voltage of the high-impedance voltage terminal Y is transfered with the gain 1 and -1 to the terminals XP and XN, respectively. This relation between the terminal voltages and currents can be described by the following matrix:

$$\begin{bmatrix} i_{\mathrm{Y}} \\ v_{\mathrm{XP}} \\ v_{\mathrm{XN}} \\ i_{\mathrm{ZP}} \\ i_{\mathrm{ZN}} \end{bmatrix} = \begin{bmatrix} 0 & 0 & 0 & 0 & 0 \\ \alpha_P & 0 & 0 & 0 & 0 \\ -\alpha_N & 0 & 0 & 0 & 0 \\ 0 & \beta_P & 0 & 0 & 0 \\ 0 & \beta_N & 0 & 0 & 0 \end{bmatrix} \begin{bmatrix} v_{\mathrm{Y}} \\ i_{\mathrm{XP}} \\ i_{\mathrm{XN}} \\ v_{\mathrm{ZP}} \\ v_{\mathrm{ZN}} \end{bmatrix}, \quad (2)$$

where $\alpha_P = 1 - \varepsilon_{VP}$, $\alpha_N = 1 - \varepsilon_{VN}$, and $\beta_P = 1 - \varepsilon_{IP}$, $\beta_N = 1 - \varepsilon_{IN}$ are the voltage and current transfer ratios of the DXCCII.

3. Proposed Voltage-Mode Fast Rectifier

The designed voltage-mode fast full-wave rectifier using single CCII and DXCCII are shown in Fig. 2. In case of the circuit solution from Fig. 2(a), the input signal v_1 is directly applied to the Y terminal of the CCII and hence the input impedance is infinitely high in theory. Assuming the structure from Fig. 2(b), the input impedance is equal to the resistance of the resistor R_1. The output resistance of both the circuit solutions is equal to R_2.

Analyzing the full-wave rectifier from Fig. 2(a), positive input voltage v_1 causes the current flow through the resistor R_1. This current is conveyed to the Z terminal of the CCII and opens the diode D_2 (the diode D_1 stays in its non-conductive state) and using DXCCII this current is on the resistor R_2 converted back to output voltage v_2. Similarly, for negative input voltage v_1, the diode D_1 and D_2 is in the ON and OFF state, respectively. Mathematically, the behavior of the full-wave rectifier can be described as follows:

$$v_2 = \begin{cases} \alpha_C \beta_C \beta_P \beta_N \cdot \dfrac{R_2}{R_1} v_1 & \text{if } v_1 > 0; \\ -\alpha_C \beta_C \beta_P \cdot \dfrac{R_2}{R_1} v_1 & \text{if } v_1 < 0. \end{cases} \quad (3)$$

Similarly, the output voltage of the full-wave rectifier from Fig. 2(b) can be expressed by the following equation:

$$v_2 = \begin{cases} \beta_C \beta_P \beta_N \cdot \dfrac{R_2}{R_1} v_1 & \text{if } v_1 > 0; \\ -\beta_C \beta_P \cdot \dfrac{R_2}{R_1} v_1 & \text{if } v_1 < 0. \end{cases} \quad (4)$$

Assuming ideal behavior of the active elements used in the full-wave rectifiers from Fig. 2 and the resistors R_1 and R_2 to be equal ($R_1 = R_2$), for both solutions the output voltage v_2 can be simply given as:

$$v_2 = |v_1|. \quad (5)$$

4. DC and RMS Error Analyses

To evaluate the accuracy of the proposed full-wave rectifier and to enable its comparison to other coming circuit solutions, the DC value transfer p_{DC} and RMS error p_{RMS} have been analyzed [26]:

$$p_{\mathrm{DC}} = \frac{\int\limits_T y_{\mathrm{R}}(t)\,\mathrm{d}t}{\int\limits_T y_{\mathrm{ID}}(t)\,\mathrm{d}t}, \quad (6)$$

$$p_{\mathrm{RMS}} = \sqrt{\frac{\int\limits_T \left[y_{\mathrm{R}}(t) - y_{\mathrm{ID}}(t)\right]^2\,\mathrm{d}t}{\int\limits_T y_{\mathrm{ID}}^2(t)\,\mathrm{d}t}}, \quad (7)$$

where the $y_{\mathrm{R}}(t)$ and $y_{\mathrm{ID}}(t)$ represent the actual and ideally rectified signal and T is the period of the rectified signal. The ideal behavior of the rectifier is characterized by the values $p_{\mathrm{DC}} = 1$ and $p_{\mathrm{RMS}} = 0$. Increasing the frequency and decreasing the magnitude of the input signal, compared to ideally rectified signal deviations of the actual output voltage $v_2(t)$ occur and p_{DC} decreases below one and p_{RMS} increases.

5. Simulation Results

To verify the behavior of the presented full-wave rectifiers, the solution from Fig. 2(a) has been further analyzed. The used CMOS implementation of DXCCII is given in Fig. 3(a) [18]. The CMOS implementation of CCII has been created from Fig. 3(a) by its proper simplification. The transistor parameters used for the simulations are taken from TSMC 0.35 μm process [27]. The aspect ratios of NMOS and PMOS transistors are $(W/L)_{1,2} = 3\ \mu\mathrm{m}/1.5\ \mu\mathrm{m}$, $(W/L)_{3,4,5,1c,2c} = 6\ \mu\mathrm{m}/1.5\ \mu\mathrm{m}$, $(W/L)_{6,7} = 5\ \mu\mathrm{m}/1.5\ \mu\mathrm{m}$, $(W/L)_{8,9,10,3c,4c} = 10\ \mu\mathrm{m}/1.5\ \mu\mathrm{m}$,

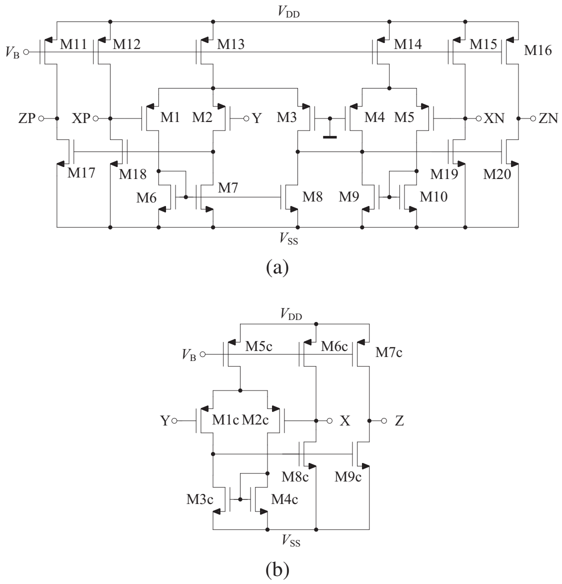

Figure 3. CMOS implementation of (a) DXCCII [18], (b) CCII

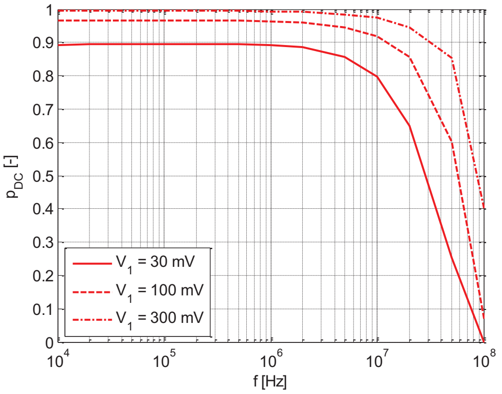

Figure 4. Transfer value p_{DC} for input signal magnitudes 30 mV, 100 mV, and 300 mV

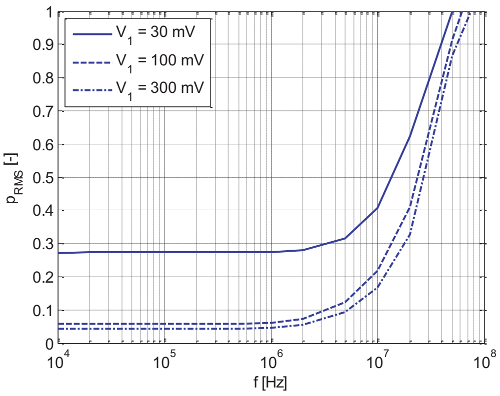

Figure 5. RMS error p_{RMS} for input signal magnitudes 30 mV, 100 mV, and 300 mV

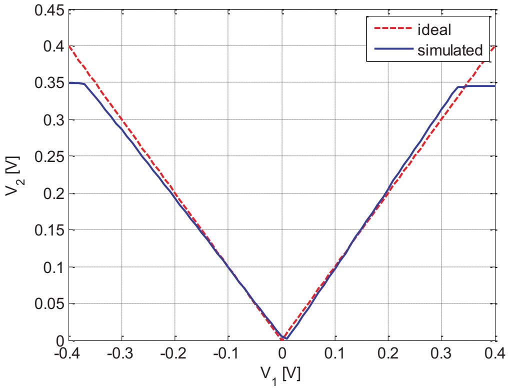

Figure 6. DC transfer characteristic of the proposed rectifier

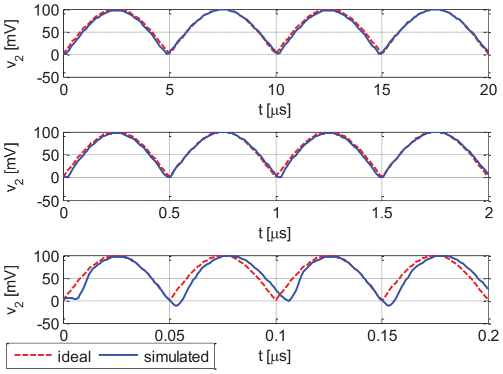

Figure 7. Transient responses for $V_1 = 100$ mV and frequencies 100 kHz, 1 MHz, and 10 MHz

$(W/L)_{11-20,5c-9c} = 30\ \mu\mathrm{m}/0.75\ \mu\mathrm{m}$. The supply voltage is ±2.5 V and bias voltage is $V_{\mathrm{B}} = 1.265$ V.

Using (6) and (7), the proposed current-mode precision rectifier has been simulated. Here, the diodes are 1PS79SB63 [28] and the resistance R_{L} was set to 1 kΩ. The simulation results of the frequency dependent DC value transfer and RMS error for chosen values of amplitudes V_1 are shown in Fig. 4 and Fig. 5. As already mentioned above, in case of ideal behavior of the full-wave rectifier, the values of p_{DC} and p_{RMS} are equal to one and zero, respectively. From Fig. 4 and Fig. 5 it can be seen that the proposed circuit behaves nearly ideally at frequencies up to 1 MHz. As the frequency of the rectified signal further increases and/or amplitude decreases distortions in the output signal $v_2(t)$ start occur and the p_{DC} decreases below one and p_{RMS} increases. Analyzing the DC transient value in Fig. 4, for the input current signal of the magnitude 30 mA, 100 mV, and 300 mV correct DC values can be achieved up to the –3 dB cutoff frequency which is 20 MHz, 32 MHz, and 63 MHz, respectively. It is obvious that for higher magnitudes of the input signal the rectifier can be used at higher frequencies. As shown in Fig. 6, the proposed circuit can be used to rectify signals of up to 350 mV magnitude. For such magnitude, correct DC values can be achieved up to frequency 83 MHz. To complete the simulations, the transient response of the rectifier for input signal magnitude $V_1 = 100$ mV and frequencies 100 kHz, 10 MHz, and 10 MHz are shown in Fig.7. The distortions of output signal $v_2(t)$ for the frequency of 1 MHz are minor. First for the frequency of 10 MHz the dynamic performance of the diodes, e.g. the time limited changes between ON and OFF states, start to be more significant, which lead to the distortions of the output signal, mainly visible in the zero-crossing area.

6. Conclusion

In this paper new circuit solutions of current conveyor based fast full-wave rectifiers working in the voltage-mode have been presented. In these structures, the CCII and DXCCII as active elements have been used. The circuits are of minimal configuration as only two diodes and two resistors are required. For the needs of application, the input impedance of the functional block can be infinitely high in theory or exactly adjusted by means of passive elements. Using the CMOS implementation of the active elements, the one of the proposed structures has been further analyzed using SPICE. Evaluating the frequency dependent DC value transfer p_{DC} and RMS error p_{RMS}, it has been shown that the circuit is feasible to operate and process signals of frequencies up to 83 MHz.

7. References

[1] U. Tietze, Ch. Schenk, and E. Gramm, ”*Electronic Circuits-Handbook for Design and Application*,” Springer, 2008.

[2] C. Toumazou and F.J. Lidgey, ”Fast current-mode precision rectifier,” *Electron. Wireless World*, vol. 93, no. 1621, pp. 1115-1118, 1987.

[3] S.J.G. Gift and B. Maundy, ”Versatile precision full-wave rectifiers for instrumentation and measurements,” *IEEE Trans Instrum. Meas.*, vol. 56, no. 5, pp. 1703-1710, 2007.

[4] C. Toumazou, F.J. Lidgey, and D.G. Haigh, ”*Analogue IC design: the current-mode approach*,” Peter Peregrinus, 1990.

[5] C. Toumazou, F.J. Lidgey, and S. Chattong, ”High frequency current conveyor precision full-wave rectifier,” *Electronics Letters*, vol. 30, no. 10, pp. 745-746, 1994.

[6] A.A. Khan, M.A. El-Ela, and M.A. Al-Turaigi, ”Current-mode precision rectification,” *Int. J. Electron.*, vol. 79, no. 6, pp. 853-859, 1995.

[7] B. Wilson and V. Mannama, ”Current-mode rectifier with improved precision,” *Electronics Letters*, vol. 31, no. 4, pp. 247-248, 1995.

[8] D. Stiurica, ”Truly temperature independent current conveyor precision rectifier,” *Electronics Letters*, vol. 31, no. 16, pp. 1302-1303, 1995.

[9] S.J.G. Gift, ”A high-performance full-wave rectifier circuit,” *Int. J. Electron.*, vol. 87, no. 8, pp. 925-930, 2000.

[10] E. Yuce, S. Minaei, O. Cicekoglu, ”Full-wave rectifier realization using only two CCII+s and NMOS transistors,” *Int. J. Electron.*, vol. 93, no. 8, pp. 533-541, 2006.

[11] S. Minaei and E. Yuce, ”A New Full-Wave Rectifier Circuit Employing Single Dual-X Current Conveyor,” *Int. J. Electron.*, vol. 95, no. 8, pp. 777-784, 2008.

[12] C. Chanapromma and K. Daoden, ”A CMOS fully differential operational transconductance amplifier operating in sub-threshold region and its application,” in *Proc. IEEE 2nd Int. Conf. Signal Proc. Systems - ICSPS 2010*, pp. V2-73–V2-77, 2010.

[13] C. Jongkunstidchai, C. Fongsamut, K. Kumwachara, and W. Surakampontorn, ”Full-wave rectifiers based on operational transconductance amplifiers,” *Int. J. Electron. Commun.* vol. 61, pp. 195-201, 2007.

[14] S. Maheshwari, ”Current controlled precision rectifier circuits,” *J. Circuits, Systems, and Computers*, vol. 16, no. 1, pp. 129-138, 2007.

[15] N. Minhaj, ”Transconductance element-based non-inverting and inverting precision full-wave rectifier circuits,” in *Proc. IEEE Int. Conf. Advantages in Computing, Control, and Telecommunication Technologies*, pp. 442-445, 2009.

[16] N. Minhaj, ”OTA-based non-inverting and inverting precision full-wave rectifier circuits without diodes,” *Int. J. Recent Trends in Engineering*, vol. 1, no. 3, pp. 72-75, 2009.

[17] N. Minhaj, ”Electronically controlled precision full-wave rectifier circuits,” in *Proc. IEEE Int. Conf. Advantages in Recent Technologies in Communication and Computing*, pp. 240-243, 2009.

[18] A. Zeki and A. Toker, ”The dual-X current conveyor (DXCCII): a new active device for tunable continuous-time filters,” *Int. J. Electron.*, vol. 89, no. 12, pp. 913-923, 2002.

[19] A. Sedra and K.C. Smith, ”A second-generation current conveyor and its application,” *IEEE Trans. Circ. Th.*, vol. 17, pp. 132-134, 1970.

[20] K.C. Smith and A., Sedra, ”The current conveyor: a new circuit building block,” *IEEE Proc.*, vol. 56, pp. 1368-1369, 1968.

[21] A. Fabre, ”Third-generation current conveyor: a new helpful active element,” *Electronics Letters*, vol. 31, no. 5, pp. 338-339, 1995.

[22] A. Fabre, O. Saaid, F. Wiest, and C. Baucheron, ”High frequency applications based on a new current controlled conveyor,” *IEEE Trans. Circuits Syst.-I*, vol. 43, no. 2, pp. 82-90, 1996.

[23] H.O. Elwan and A.M. Soliman, ”Novel CMOS differential voltage current conveyor and its applications,” *IEE Proc. Circuits, Devices, Systems*, vol. 144, no. 3, pp. 195-200, 1997.

[24] W. Surakampontorn and K. Kumwachara, ”CMOS-based electronically tunable current conveyor,” *Electronics Letters*, vol. 28, no. 14, pp. 1316-1317, 1992.

[25] I.A. Awad and A.M. Soliman, ”Inverting second generation current conveyors: the missing building blocks, CMOS realizations and applications,” *Int. J. Electron.*, vol. 86, no. 4, pp. 413-432, 1999.

[26] D. Biolek, V. Biolkova, and Z. Kolka, ”AC analysis of operational rectifiers via conventional circuit simulators,” in *Proc. WSEAS Transactions on Circuits and Systems*, vol. 3, no. 10, pp. 2291- 2295, 2004.

[27] N. Herencsar, J. Koton, K Vrba, A. Lahiri, U.E. Ayten, and M. Sagbas, ”A new compact CMOS realization of sinusoidal oscillator using single modified CBTA,” in *Proc. 21st Int. Conf. Radioelektronika*, Brno, Czech Republic, 2011.

[28] Datasheet 1PS79SB63, Philips Semiconductors, Rev. 02, Dec 2004.